Characterization of Fer1L6 lipid binding properties and its expression in cell cycle

by
Trisha Chau

A THESIS

submitted to

Oregon State University

Honors College

in partial fulfillment of
the requirements for the
degree of

Honors Baccalaureate of Science in Biochemistry and Molecular Biology
(Honors Scholar)

Presented May 7, 2018
Commencement June 2018

AN ABSTRACT OF THE THESIS OF

Trisha Chau for the degree of Honors Baccalaureate of Science in Biochemistry and Molecular Biology presented on April 20, 2018. Title: Characterization of Fer1L6 lipid binding properties and its expression in cell cycle

Abstract approved:_____

Colin Johnson

Ferlins are a family of calcium-sensitive proteins involved in fusion and fission membrane trafficking events. There are six ferlin members: dysferlin, otoferlin, myoferlin, Fer1L4, Fer1L5, and Fer1L6. Previous research shows the first three ferlins play a pathophysiological role in humans, while the other three remain uncharacterized. Fer1L6 is one of the three uncharacterized proteins, but studies in our lab suggest that it may play a role in muscle development in zebrafish. Fer1L6 contains five C2 domains that bind calcium ions and target the protein to membranes. However, to understand how Fer1L6 deficiency disrupts normal muscle development, we must understand how the protein interacts with lipids. To gain insight into how Fer1L6 functions, laurdan fluorescence assays, co-sedimentation assay, and cell culture studies were performed.

Our assays show that the C2 domains of Fer1L6 exhibit electrostatic and hydrophobic interactions similar to those seen in the other ferlins. In addition, the domains of Fer1L6 prefer to bind to negatively charged phospholipids, implying that Fer1L6 may localize to plasma membrane or Golgi apparatus. Our study also indicates Fer1L6 is highly expressed in the G_2 stage of the cell cycle. Understanding each domain's lipid-binding affinity, our next step is to construct truncated and full-length Fer1L6 and investigate their effects on lipid binding.

Key Words: Fer1L6, membrane-binding proteins, calcium sensitive, fluorescence, co-sedimentation, C2C12

Corresponding e-mail address: trchau8@gmail.com

Characterization of Fer1L6 lipid binding properties and its expression in cell cycle

by
Trisha Chau

A THESIS

submitted to

Oregon State University

Honors College

in partial fulfillment of
the requirements for the
degree of

Honors Baccalaureate of Science in Biochemistry and Molecular Biology
(Honors Scholar)

Presented May 7, 2018
Commencement June 2018

Honors Baccalaureate of Science in Biochemistry and Molecular Biology project of Trisha Chau presented on May 7, 2018.

APPROVED:

_____
Colin Johnson, Mentor, representing Department of Biochemistry and Biophysics

_____
Rick Cooley, Committee Member, representing Department of Biochemistry and Biophysics

_____
Kari van Zee, Committee Member, representing Department of Biochemistry and Biophysics

_____
Toni Doolen, Dean, Oregon State University Honors College

I understand that my project will become part of the permanent collection of Oregon State University, Honors College. My signature below authorizes release of my project to any reader upon request.

_____
Trisha Chau, Author

ACKNOWLEDGEMENTS

I would like to thank my mentor, Dr. Colin Johnson, for taking me under his wings since my freshman year. I would like to thank my fellow lab mates for their patience and contributions: Dr. Nicole Hams, Aayushi Manchanda, Dr. Josephine Bonventre, Dr. Sara Codding, Dr. Murugesh Narayanappa, Blake Hakkila, Shauna Otto, James Miyasaki, and Tanushri Kumar. Thank you to Kayla Jara for assisting me with the cell culturing. I would like to give big thanks to my mentor, Dr. Chelsea Wolk, who both trained and guided me in the early parts of my research. Thank you to Dr. Kari van Zee, Dr. Viviana Perez, Dr. Indira Rajagopal, LeAnn Adam and Wanda Crannell for their guidance in life. I would also like to thank URSA-ENGAGE, URISC, SURE, and CURE for funding my work.

Last, but most importantly, I would like to thank my family and friends for their continual support in my happiness of pursuit. To my family, thank you for teaching me to be humble, to stand up for myself and for others, and to know that I cannot have a cake and eat it too. Thank you to my friends, Kevin Bishop, Dani Stevens, Emma Chilcote, Arvin Halim, Makayla Lindemann, Jon Holland, and my OSU Taekwondo family for their support.

INTRODUCTION

Fer1L6 belongs to a family of calcium-sensitive, membrane-trafficking proteins called ferlins (200-240kDa). The ferlin family in mammals is composed of six total proteins, each comprised of five to seven tandem C2 domains with a transmembrane domain at the C-terminal end. Originally identified in protein kinase C isoform, C2 domain is a calcium-binding motif and is composed of eight beta-stranded sheets.[1] The C2 domains are found in many eukaryotic proteins and function in different intracellular processes like generating lipid-second messengers and membrane trafficking. As of today, C2A domain of otoferlin is the only C2 domain successfully crystallized (Figure 1a).[2] Though the C2 domain has calcium-binding loops at both the N- and C-terminals, all C2 domains are not regulated by calcium, suggesting some C2 domains may have lost their ability to bind to calcium.[2] Though Fer1L6 contains five C2 domains, it is not known if all of the domains are sensitive to calcium (Figure 1b).

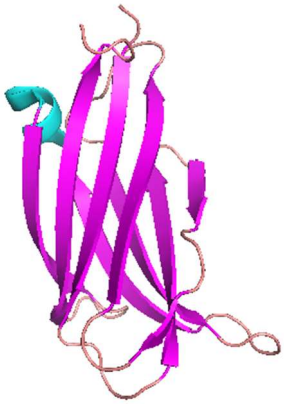

a.

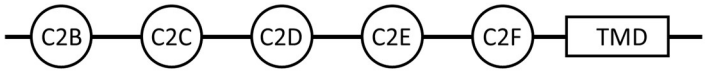

b.

Figure 1. Structure of C2 domain and Fer1L6. Figure 1a shows the crystallized structure of otoferlin C2A domain (PDB: 3L9B), comprised of 8 beta-strands and a small helical segment. Figure 1b shows a schematic diagram of Fer1L6 containing five C2 domains (C2B-C2F) and a transmembrane domain.

Despite structural similarities, ferlins have diverse functions.[3] Dysferlin (Fer1L1) is responsible for skeletal muscle membrane repair, and myoferlin (Fer1L3) is a key regulator in preventing the development of breast cancer.[4,5] Otoferlin (Fer1L2) is involved with releasing neurotransmitters in hair cell neruons.[6] Fer1L4 is a non-coding RNA associated with gastric cancer development, and Fer1L5 mediates myoblast fusion.[7,8] However, the functions of Fer1L6 have not been well-characterized. Since the rest of mammalian ferlins have been characterized to a certain extent, it is of interest for us to characterize the least well-known ferlin, Fer1L6.

The ferlin family is divided into two subgroups based on the presence or absence of a DysF domain, where dysferlin, and myoferlin, and Fer1L5 has this domain.[9] Studies have suggested DysF domain is a binding site for caveolin-3, which is involved in lipid invagination.[10] Although Fer1L6 lacks a DysF domain like Fer1L4, studies suggest it may play a role in development, similar to myoferlin which does contain DysF.[11,12] Fer1L6 has been shown to localize around the nucleus and plasma membrane in C2C12 cells. Fer1L6 is shown to co-localize with two SNARE proteins: SNAP-23 and syntaxin-4, which suggested Fer1L6 plays a role in vesicle trafficking of the cells.[13] Other studies have shown Fer1L6 is highly expressed in the heart, kidneys, and stomach and is not expressed well in the lungs, liver, pancreas, thymus, and the colon. It is interesting to note that it was not expressed in skeletal

muscles.[14] Overall, there have only been a few studies that have characterized the properties of Fer1L6, and more studies still need to be done to understand its phenotypic role.[3,15,16]

Since our data has suggested that Fer1L6 also plays a role in membrane trafficking, it is of interest to investigate how each domain of Fer1L6 binds to phospholipid membrane in order to better characterize this ferlin gene. Previous work used laurdan fluorescence assay to study the binding of C2 domains from myoferlin, dysferlin, and otoferlin.[17] Since these C2 domains bind to phosphatidylcholine (PC) and phosphatidylserine (PS) to some degree, we wanted to use the same assay to investigate the binding affinity of Fer1L6's C2 domains. The laurdan fluorescence assay was expanded to test the lipid-binding affinities of the C2 domains in high salt conditions and to test when the domains were most sensitive to calcium. Co-sedimentation assay was also used to obtain information about the lipid-binding interactions of the C2 domains. Moreover, a recent study suggested there was an association of Fer1L6 with the cell cycle, so qPCR was used to quantify the amount of Fer1L6 expressed in C2C12 cells after they were inhibited by Lovastatin.

It is expected that the domains of Fer1L6 will bind more to POPC/POPS than just POPC since C2 domains generally have a greater affinity towards acidic lipids. In addition, it is expected that increased in salt concentration would disrupt the interaction of the C2 domain to the membrane, but an increase in calcium concentration would increase the binding affinity of the domains to the phospholipid membrane due to increase in electrostatic interaction.

By characterizing Fer1L6, we can compare its functions and characteristics to what is already known about the other the other five ferlins. This would provide us with a better wholistic picture of the ferlin family.

MATERIALS AND METHODS

Materials

Common reagents and primers were purchased from New England BioLabs (Ipswich, MA), Sigma-Aldrich (St. Louis, MO), ThermoFisher Scientific (Waltham, MA), Qiagen (Hilden, Germany), and Research Product International (Mount Prospect, IL). Puc57 vector was purchased from GenScript (Piscataway, NJ). High density nickel agarose beads were obtained from Gold Biotechnology (St. Louis, MO). Lipids, membrane, extruder, and syringes were obtained from Avanti Polar Lipids (Alabaster, AL). Lovastatin was obtained from AdipoGen Life Sciences (San Diego, CA).

Cloning Fer1L6 Domains

DH5α *E. coli* cells containing pMCSG9 vector were grown in lysogeny broth (LB) containing ampicillin (0.1 mg/mL) for 18 hours at 37°C. In addition, *E. coli* DH5α cells containing pUC57-Fer1L6 was grown in kanamycin-containing (0.05 mg/mL) LB under the same conditions. Both plasmids were purified using QIAprep Spin Miniprep Kit. SSPI-HF enzyme was used to digest the pMCSG9 vector, and the vector was run on agarose gel before purifying the vector with QIAEX II Gel Extraction Kit.

pUC57-Fer1L6 was used as a template for amplification of each Fer1L6 domain. Forward and reverse primers were designed to amplify the 5' and 3' coding sequence of each domain: C2B (amino acids 77-174), C2C (amino acids 237-344), C2D (amino acid 818-926), C2E (amino acids 1007-1090), and C2F (amino acids 1349-1450). LIC sequence was added to both ends of the forward and reverse primers, so the amplicons would adhere to SSPI/T4-treated pMCSG9 vector. The amplicons of each domain were amplified and then purified via PCR purification kit. Both vector and amplicons were mixed and ligated with T4 DNA ligase. The plasmids were then transformed into *E. coli* DH5α cells. The sequence in the colonies were checked by GenScript before being retransformed into *E. coli* BL21 cells.

Protein Expression

For each his-tagged MBP Fer1L6 domain, the BL21 cells were grown in LB for 18 hours at 250 rpm at 37°C. The culture (5 mL) was then transferred to 1.5 L fresh LB and were incubated at 37°C until their optical density reached 0.6. The cells were induced with 1 mM isopropyl β-D-1-thiogalactopyranoside (IPTG) before being incubated for four hours longer. The cells were centrifuged at 4,000 rpm before using a microfluidizer to lyse the cells with lysis buffer (20 mM phosphate, 150 mM NaCl, 10 mM imidazole, pH 7.5), Pepstatin A (1 μg/mL), leupeptin (1 μg/mL), and phenylmethane sulfonyl fluoride (PMSF) (1 mM) were added. The cell lysate was frozen at -80°C for storage overnight and was then thawed in a 37°C bath. The cell lysate was centrifuged at 2,000 rpm until all cellular components formed a pellet. The soluble fractions were then added to high density nickel agarose beads and washed with 20 bed volumes of lysis buffer before the domains were eluted with two bed

volumes of elution buffer (20 mM phosphate, 150 mM NaCl, 500 mM imidazole, pH 7.4). The proteins were dialyzed for at least sixteen hours with 1x phosphate buffered saline (PBS) (20 mM phosphate, 150 mM NaCl, pH 7.4) at 4°C.

Small Unilamellar Vesicle (SUV) Preparation

1-palmitoyl-2-oleoyl-sn-glycero-3-phosphocholine (POPC), 1-palmitoyl-2-oleoyl-sn-glycero-3-phospho-L-serine (POPS), and laurdan dissolved in chloroform were mixed together to the desired ratio (97.5% POPC/2.5% laurdan and 48.75% POPC/48.75% POPS/2.5% laurdan). The contents were put under vacuum until the solvent evaporated. The lipids were then rehydrated with 1x PBS until the concentration was 2 mM and then extruded to form vesicles using a 50 nm-cutoff membrane and a polycarbonate filter.

Protein Fluorescence Measurements

Using a QM-40 fluorometer with Glan Thompson polarizers (Photon Technology International, Birmingham, NJ), laurdan fluorescence was measured at 37°C. All fluorescent mixtures were in 1x PBS (pH 7.5). The fluorophore laurdan was excited at wavelength 350 nm. Generalized polarization (GP) value was measured based on the following equation: $GP = (I_{430} - I_{480}) / (I_{430} + I_{480})$, where I_{430} and I_{480} are the intensities emitted by laurdan at wavelengths 430 nm and 480 nm, respectively.

Co-sedimentation

Mixtures consisted of 5 μM of protein, 1 mM of SUVs, and nitrobenzoxadiazole (NBD) in 1x PBS buffer with either calcium (100 μM or 1 mM) or ethylenediaminetetraacetic acid (EDTA) (1 mM). The mixtures were incubated for

30 minutes at 21°C. They were centrifuged at 85,000 xg for 45 minutes at 4°C in a TA-100 ultracentrifuge (Beckmann Instruments). Pellets were resuspended in 10% SDS, and for each sample, both the pellet and supernatant were run on 12% SDS-PAGE gel.

Cell culture

C2C12 cells were grown on 12-well plates at 37°C with 5% CO_2 humidity until they were 70% confluent. The cells were washed with 1x PBS and media (1x DMEM, 10% Fetal Bovine Serum, and 1.0% Penicillin Streptomycin) was changed prior to adding Lovastatin, which was dissolved in 75% ethanol. Serial dilutions of lovastatin were made to various final concentrations (5 μM, 10 μM, 20 μM, 40 μM, and 50 μM). C2C12 cells were treated with RNAzol prior to collecting the cells at 6, 12, and 18 hours after treatment and were frozen down at -80°C.

RNA Isolation and conversion to cDNA

Cells were homogenized in 200 μL ultra-pure distilled water. Homogenate was vigorously shaken for 15 seconds before letting the cells sit at 21°C for 15 minutes. The cells were spun at 12,000 rcf for 15 minutes. 600 μL of supernatant was mixed with an equal volume of isopropanol. Cells were incubated at 21°C for another 15 minutes before spinning for 10 minutes at 12,000 rcf. Supernatant was removed and 500uL of 75% ethanol was added. Solution was spun for 3 minutes at 8,000 rcf, and supernatant was decanted. Another 100 μL of 75% ethanol was added before spinning again. Supernatant was decanted and RNA was left to air dry before rehydrating with ultra-pure distilled water. RNA concentrations were diluted to 200 ng/μL. The respective cDNAs were created using Applied Biosystem reagents and

protocol. qPCR was conducted using 2X SYBR 6 Green master mix (Life Technologies). Gene-specific primers were mixed with their respective cDNAs in a 20 μL reaction. cDNAs were amplified. ΔΔ CT was calculated to determine the concentration of each cDNA.

RESULTS/DISCUSSION

Fluoresence assay shows Fer1L6 exhibits electrostatic interactions

We first used laurdan fluorescence assay to determine how each Fer1L6 domain binds to lipid membranes. We mixed the membrane and the domain of interest with a small, fluorescent membrane probe called laurdan (Figure 2a). Laurdan absorbs at 430 nm because it takes a certain amount of energy to excite electrons at ground state to an excited state, and the energy absorption is unique to a given molecule and transition. The energy emitted is at a longer wavelength, specifically at 480 nm (Figure 2b). Using the equation as previously described, we calculated the normalized intensity ratio called generalized polarization (GP) values for each sample. The GP value ranges from -1 (most disordered state) to +1 (most ordered state). If the Fer1L6 domains bind deeply into the membrane vesicles, the lipids become more packed and a more positive value would be expected. A negative value indicates the domain is not interacting with the membrane vesicles. No units are given for GP values because the units cancel out when calculating the GP values; therefore, the units provided are arbitrary.

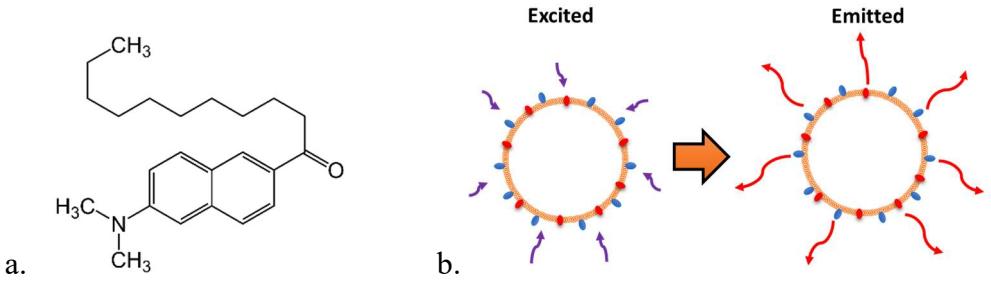

Figure 2. Laurdan fluorescence assay diagrams. Figure 2a shows the molecular structure of laurdan, a fluorescent probe used to measure binding of the domains of Fer1L6 with phospholipid membranes. Figure 2b is a schematic diagram of how fluorescence assay works. The laurdan embedded in the membrane is excited at a wavelength of 350 nm and then emits energy at wavelength of 430 or 480 nm. The blue and red ovals represent laurdan and C2 domain, respectively.

In the first set of fluorescence assay, we tested the binding of the domains to two different compositions of membranes. The first membrane composition was composed entirely of POPC, and the second composition was composed of POPC and POPS. Since C2 domain had preference for acidic lipids, the addition of POPS to POPC would increase the likelihood of binding. Comparing the GP values of our first experiment, we would expect negative values, which indicated no binding to the membranes, for our solutions containing no proteins or just MBP (Figure 3). For solutions containing just POC lipids, domains C2B and C2C bind to POPC and were calcium independent. Domains C2E and C2F did not bind to POC even in the presence of calcium, and domain C2D bind to POPC only in the presence of calcium. In a mixture of POPS and POPC, we saw similar trends except domains C2E and C2F did bind to the vesicles but were still not calcium dependent.

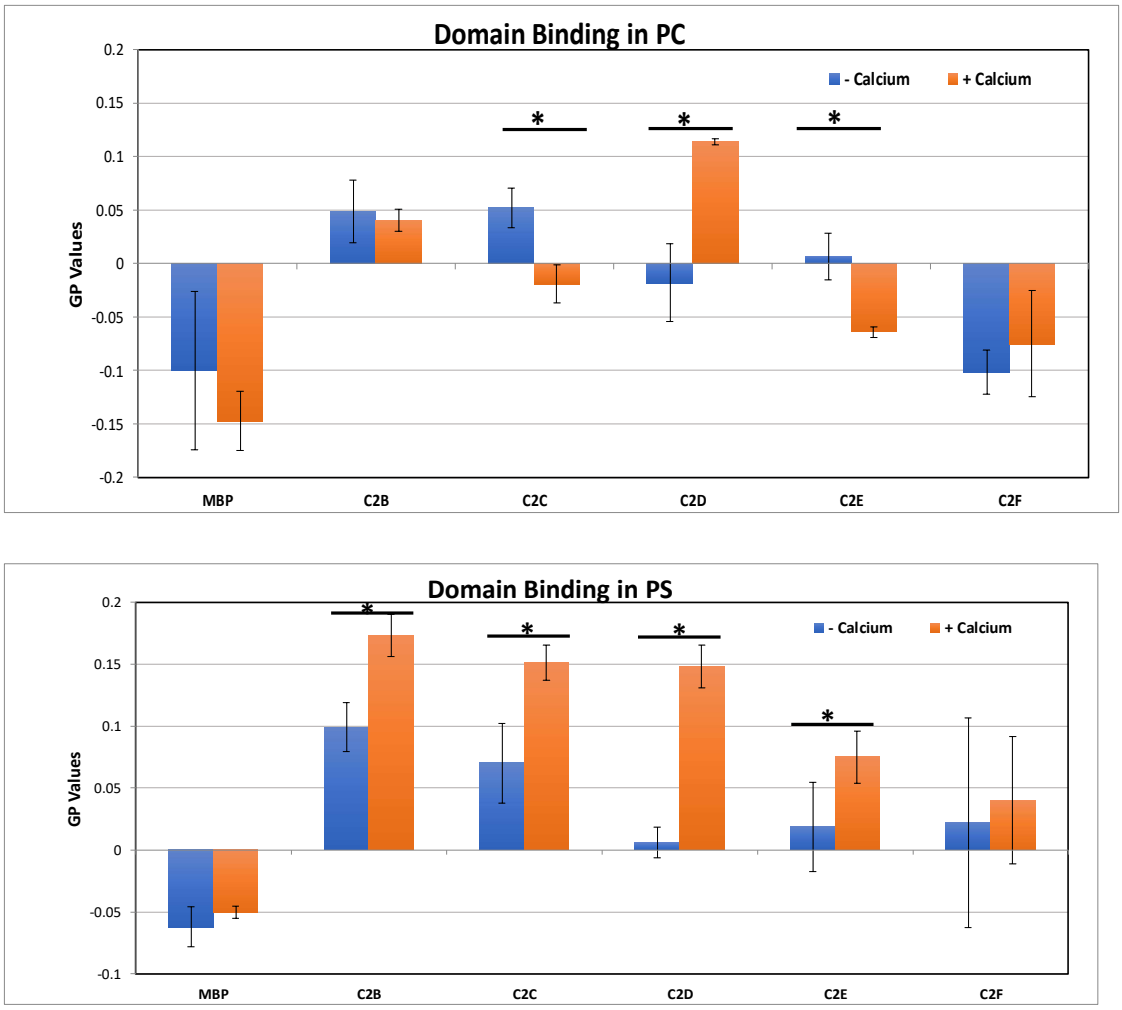

Figure 3. Binding of Fer1L6 on membranes. Binding of Fer1L6 to membrane vesicles in the absence or presence of calcium. Mixture contained 5 μM of one Fer1L6 domain, 5 μM of lipid (48.75% POPC/48.75% POPS/2.5% laurdan or 97.5% POPC/2.5% laurdan), 100 μM of EDTA or 0.25 mM of $CaCl_2$, and 137 mM of NaCl. Total volume was 60 μL. N=3. *, $p<0.05$.

From our results, we observed that domains C2B and C2C bounded to lipids regardless of the conditions. However, domain C2C did not bind to POPC in the presence of calcium. In the presence of calcium, all domains would bind to the POPS/POPC lipids, suggesting some of the N-terminal domains bind to lipid via hydrophobic interactions. To verify this hypothesis, we used the same fluorescence

assay and tested the binding at a high salt concentration versus physiological salt condition (137 mM NaCl).

High salt concentration suggest Fer1L6 exhibits hydrophobic interactions

If the domains solely interacted in an electrostatic manner, then a high salt concentration of 500 mM NaCl would disrupt the binding of the domains to the membrane vesicles, resulting in negative GP values. However, high salt did not significantly change membrane binding (Figure 4). For domains C2D and C2E, we saw an increase in binding in the presence of high amount of salt as opposed to physiological conditions in the absence of calcium. This result did not support our hypothesis regarding the domains of Fer1L6 solely rely on electrostatic interactions. Instead, the result suggested that the domains of the ferlin also interact with the lipid through hydrophobic interactions, where nonpolar amino acids avoid interacting with polar solvents by interacting with other nonpolar molecules.

It is also possible that salt destabilized domain C2B by interfering with the intramolecular non-covalent interactions, such as hydrogen bonds, van der Waals forces, and hydrophobic forces. Though it is also possible for salt to stabilize the N-terminal domains by interacting with the hydration shell around the protein. This would reduce the unfavorable thermodynamic interaction, and the domains would have a greater affinity towards the membrane.

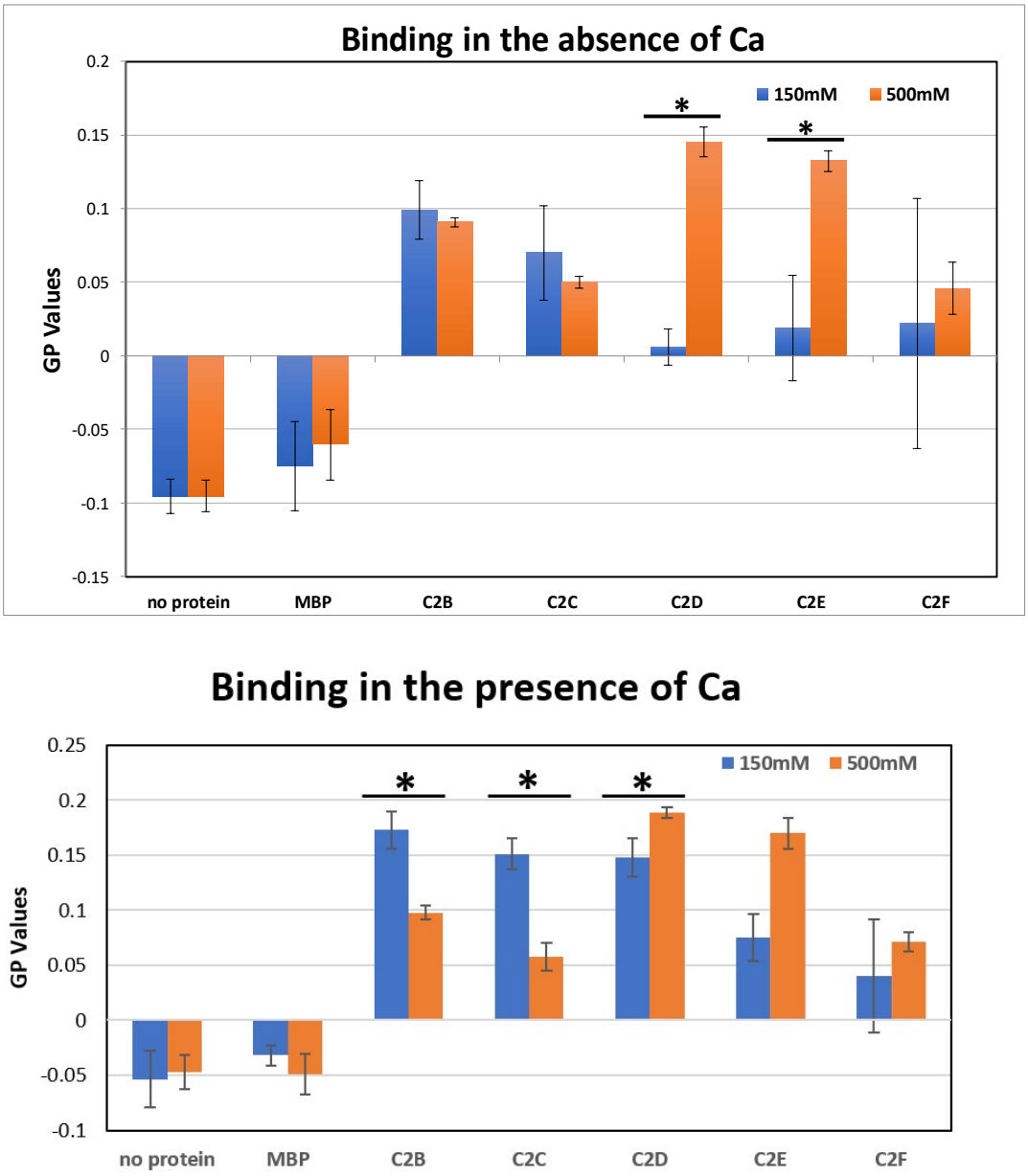

Figure 4. Effects of NaCl on the binding of Fer1L6. Domains of Fer1L6 binding to phospholipids in the presence of high salt. High salt concentration was defined at 500 mM NaCl, and physiological salt concentration was defined at 137 mM NaCl. All mixtures contained 5 μM of the respective proteins and 5 μM of the lipid (48.75% POPC/48.75% POPS/2.5% laurdan). Total volume was 60 μL. N=3. *, $p<0.05$.

Intracellular calcium concentrations ranges widely, from 10^{-7} M to 10^{-5} M calcium. When determining the preferences of Fer1L6 domains to the lipid, 0.25 mM

of calcium were used. However, we have yet to determine at what concentration of calcium causes the domains to bind most to the membrane. From our data, we saw both C2E and C2F bind to POPC/POPS vesicles the most at 100 µM of calcium (Figure 5). Therefore, it was interesting to note that the binding was not directly or indirectly proportional to the concentration of calcium in solution. Rather, binding was dependent on a specific concentration of calcium.

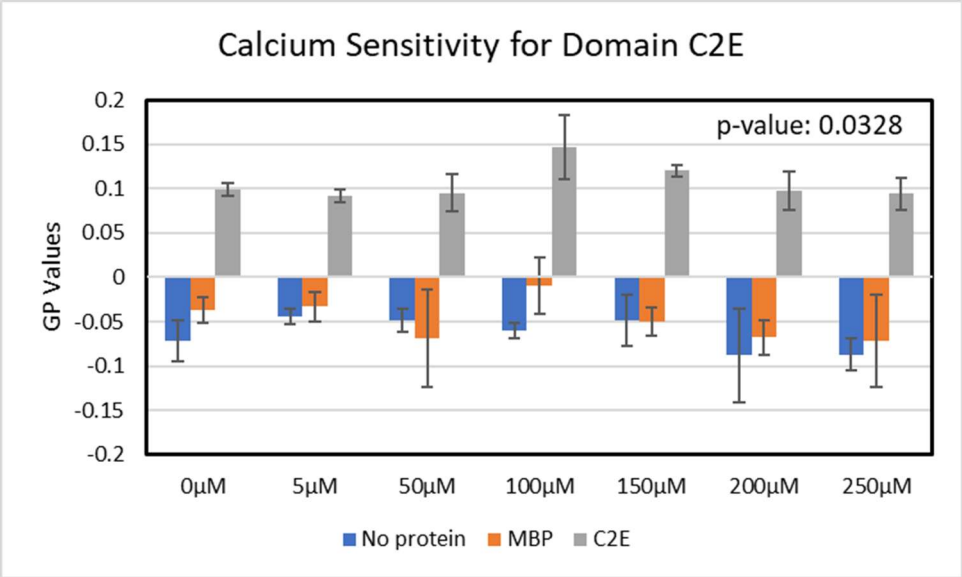

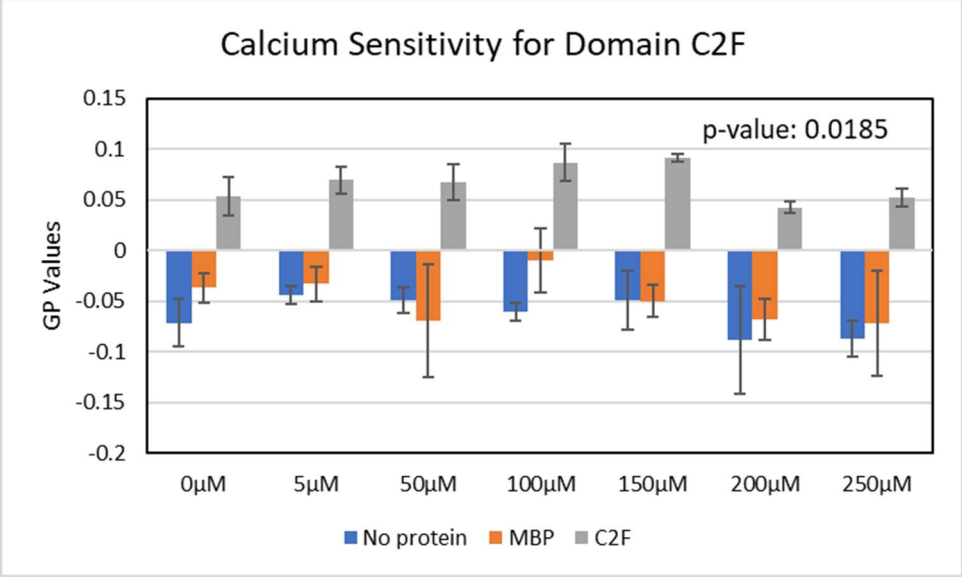

Figure 5. Effects of calcium on binding analysis. Binding affinities of domains C2E and C2F at various calcium concentrations. Each mixture consists of 5 μM of the respective protein, 5 μM of lipids (48.75% POPC, 48.75% POPC/POPS, 2.5% Laurdan), 150 μM of NaCl, and a specific amount of calcium. Total volume is 60 μL. N=3. *, $p<0.05$.

Domains of Fer1L6 demonstrates different affinities to lipid

Co-sedimentation assay was performed to qualitatively determine whether lipid binding is calcium dependent. High speed centrifugation was used to separate the particles based on their sizes, shapes, and densities (Figure 6). Using a fixed angle rotor where the tubes or placed at a slight angle, the particles would have a shorter distance to travel before pelleting as opposed to a swinging bucket rotor. At a speed of 85,000 rpm, the lipid would pellet to the bottom of the tube with or without the domains imbedded in the membrane of liposomes. If the protein bind to the lipid, the protein would pellet with the lipid. Otherwise, the protein would stay in the supernatant while the lipid pelleted to the bottom of the tube. Running the pellets and the supernatants on the gel, the bands indicated the presence of the protein, and the intensity of the band correlated to the concentration of the protein.

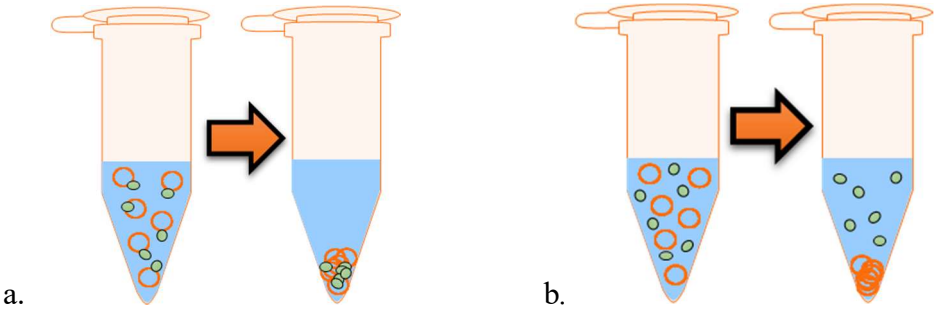

Figure 6: Schematic diagram of co-sedimentation assay. Figure 6a shows if the domain binds to the lipid, the protein would be pulled down with the lipid after high centrifugation.

However, figure 6b shows if the domain does not bind to the lipid, then only the lipid is pulled down, and the protein stays in the supernatant.

When the domains were run with just POPC, domains C2D and C2F bind to lipid independent of calcium (Figure 7). Domains C2B, C2C, and C2E only bounded to POPC to some degree at a high concentration of calcium. When testing the binding of the protein to 50% POPC/50% POPS, all of the domains, except for domain C2E, bind to the lipid in the absence of calcium. Though the results slightly differ from the fluorescence experiments, a higher concentration of lipid was used for the co-sedimentation assay. This suggested that Fer1L6 had a higher affinity towards a higher concentration of lipid, and the addition of calcium had little effect on the protein's binding.

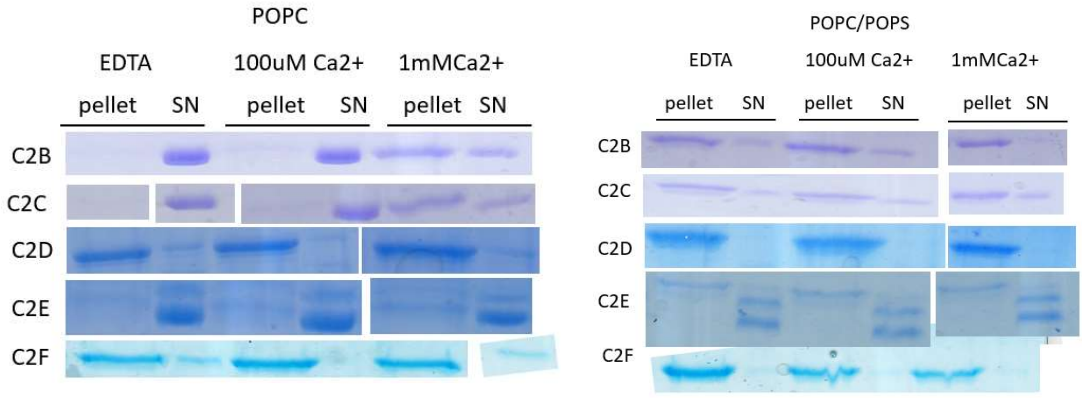

Figure 7. Co-sedimentation of Fer1L6. Co-sedimentation of all domains of Fer1L6. Mixture consisted of 5 μM of a domain, 1 mM of lipid, and nitrobenzoxadiazole (NBD). Solution either 1 mM of EDTA, 100 μM, or 1 mM of calcium. N=3.

Fer1L6 is highly expressed at the G_2 stage

A previous study observed a possible association between Fer1L6 and the cell cycle. To test this hypothesis, a mouse muscle myoblast line called C2C12 was used to measure the amount of Fer1L6 at each stage of the cell cycle. Since the cultured

cells were naturally at different stages of the cell cycle, it was necessary to synchronize all of the cells to a specific stage before quantifying the amount of Fer1L6. Therefore, a kinase inhibitor called Lovastatin was used to inhibit the cells at G_1 of the cell cycle.[18] It arrested cells at G1 phase by acting as a cyclin-dependent kinase inhibitor. Since cyclins controlled the cell cycle by activating cyclin-dependent kinases, the concentrations of different cyclins were also measured to confirm the cells were synchronized. Since the doubling time of C2C12 was 12 hours, we treated the cells for 18 hours with 50 μM of Lovastatin. qPCR was then run and ΔΔCT was determined for some of the cyclins and for Fer1L6 (Figure 8).

Different cyclins are abundant at different stages of the cell cycles. Cyclin E2 reaches its peak at the G_1 stage of the cell cycle. Cyclins B1 and B2 are abundant during the late G_2 stage of the cell cycle, and the concentration of cyclin A2 is the highest at the S stage. Lovastatin would inhibit the cells at the G_1 stage, so we expected more cyclin E2 to be present as the concentration of Lovastatin increased. We also expected less cyclins B1, B2, and A2 because a greater concentration of Lovastatin would exert a greater inhibition on the cells. Our data showed as the concentration of Lovastatin increased, so did the concentrations of cyclins B1, B2, and A2. These data trends observed did not coincide with our hypothesis. This observed trend can be explained that Lovastatin inhibited the cells at G_2 since the dose may be too low.[19] Therefore, if the C2C12 cells were actually inhibited at G_2 instead of G_1, then Fer1L6 was highly expressed at the G_2 stage of the cell cycle.

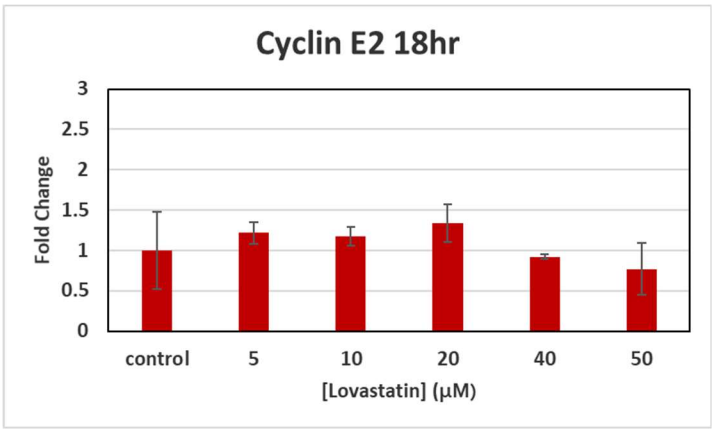
Cyclin E2 18hr
Fold Change
3
2.5
2
1.5
1
0.5
0
control
5
10
20
40
50
[Lovastatin] (µM)

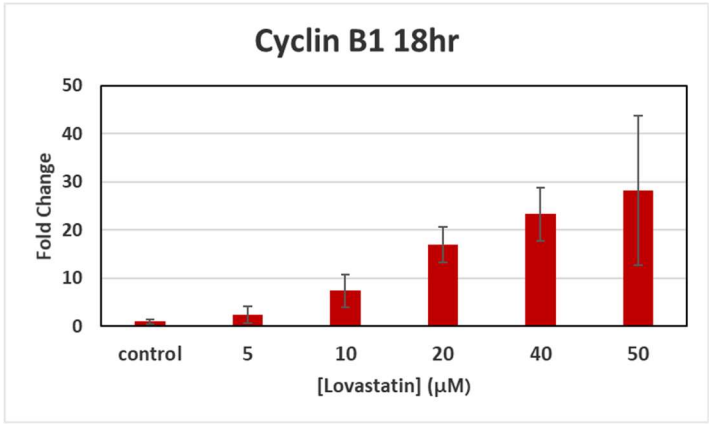
Cyclin B1 18hr
Fold Change
50
40
30
20
10
0
control
5
10
20
40
50
[Lovastatin] (µM)

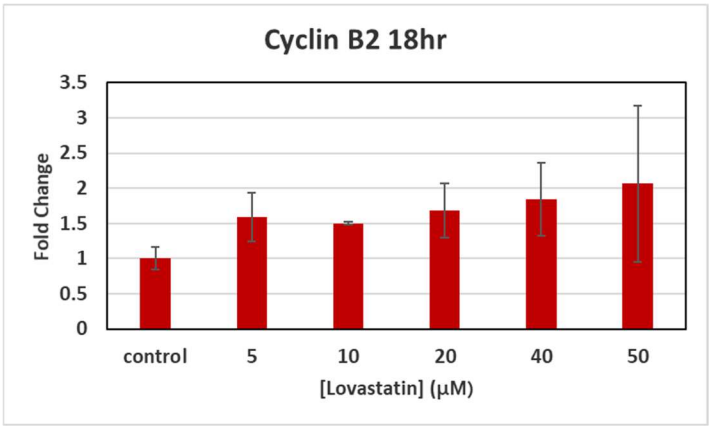
Cyclin B2 18hr
Fold Change
3.5
3
2.5
2
1.5
1
0.5
0
control
5
10
20
40
50
[Lovastatin] (µM)

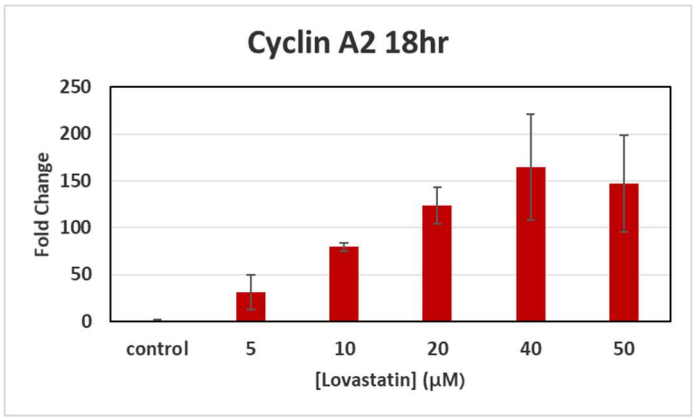

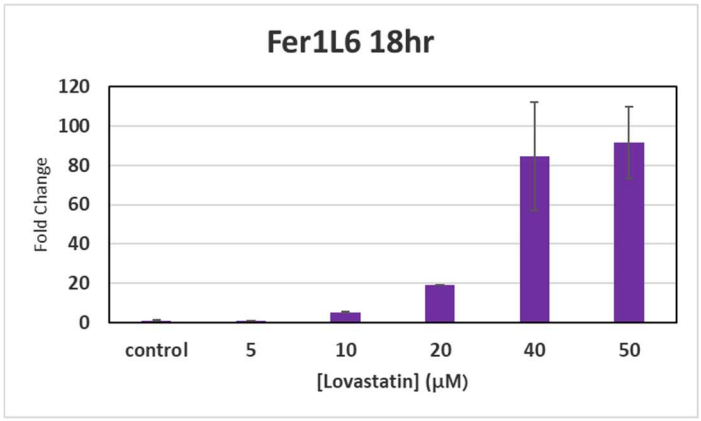

Figure 8. ΔΔ CT graph analysis. Fold changes were calculated using ΔΔ CT to determine the amount of mRNA expressed by C2C12 cells. Cells were treated for 18 hours with Lovastatin. N=2.

CONCLUSION

Studies have shown Fer1L6 localized at the trans Golgi/recycling endosomes and at the plasma membrane.[3] However, little studies have investigated how Fer1L6 localized to these compartments. Laurdan fluorescence assays assessed the binding affinities of Fer1L6. Results showed Fer1L6 generally had a greater binding affinity for negatively-charged membrane in the presence of calcium than without calcium. The increased in GP value was likely due to the addition of electrostatic interaction. Salt concentration was increased to test the binding interactions of Fer1L6. In the

absence of calcium, the increased salt concentration resulted in a greater binding affinity between N-terminal domains and negatively-charged phospholipids. In the presence of calcium, a decrease in binding affinity between the C-terminal domains and the membrane was observed, but the GP value increased for domain C2D under these conditions. Future work includes constructing full-length and truncated Fer1L6 and investigate their lipid-binding interactions.

Our next studies suggested the domains are most sensitive to calcium when it is about 100 μM. Co-sedimentation assay showed all of the domains, except for domain C2E, bind to 50% POPC/50% POPS in the absence of calcium, and domains C2B, C2C, and C2E bind to just POPC in the presence of calcium. The 200-fold increase in lipid concentration would force the domains to bind to the membrane due to a higher presence of lipid. Lastly, cell culture studies showed Fer1L6 is abundant in the G2 phase of the cell cycle.

(1) Newton, A. C. Protein Kinase C: Seeing Two Domains. *Current Biology*. 1995, pp 973–976.
(2) Nalefski, E. A.; Falke, J. J.; Nalefski, E. A.; Falke, J. J. The C2 Domain Calcium-Binding Motif : Structural and Functional Diversity. *Protein Sci.* **1996**, *5* (12), 2375–2390.
(3) Redpath, G. M. I.; Sophocleous, R. A.; Turnbull, L.; Whitchurch, C. B.; Cooper, S. T. Ferlins Show Tissue-Specific Expression and Segregate as Plasma Membrane/Late Endosomal or Trans-Golgi/Recycling Ferlins. *Traffic* **2016**, *17* (3), 245–266.
(4) Therrien, C.; Dodig, D.; Karpati, G.; Sinnreich, M. Mutation Impact on Dysferlin Inferred from Database Analysis and Computer-Based Structural Predictions. *J. Neurol. Sci.* **2006**, *250* (1–2), 71–78.
(5) Bansal, D.; Miyake, K.; Vogel, S. S.; Groh, S.; Chen, C.-C.; Williamson, R.; McNeil, P. L.; Campbell, K. P. Defective Membrane Repair in Dysferlin-Deficient Muscular Dystrophy. *Nature* **2003**, *423* (6936), 168–172.
(6) Turtoi, A.; Blomme, A.; Bellahcene, A.; Gilles, C.; Hennequiere, V.; Peixoto, P.; Bianchi, E.; Noel, A.; De Pauw, E.; Lifrange, E.; et al. Myoferlin Is a Key Regulator of EGFR Activity in Breast Cancer. *Cancer Res.* **2013**, *73* (17), 5438–5448.
(7) Roux, I.; Safieddine, S.; Nouvian, R.; Grati, M.; Simmler, M. C.; Bahloul, A.; Perfettini, I.; Le Gall, M.; Rostaing, P.; Hamard, G.; et al. Otoferlin, Defective in a Human Deafness Form, Is Essential for Exocytosis at the Auditory Ribbon Synapse. *Cell* **2006**, *127* (2), 277–289.
(8) Song, H.; Sun, W.; Ye, G.; Ding, X.; Liu, Z.; Zhang, S.; Xia, T.; Xiao, B.; Xi, Y.; Guo, J. Long Non-Coding RNA Expression Profile in Human Gastric Cancer and Its Clinical Significances. *J. Transl. Med.* **2013**, *11* (1), 1–10.
(9) Posey, A. D.; Pytel, P.; Gardikiotes, K.; Demonbreun, A. R.; Rainey, M.; George, M.; Band, H.; McNally, E. M. Endocytic Recycling Proteins EHD1 and EHD2 Interact with Fer-1-like-5 (Fer1L5) and Mediate Myoblast Fusion. *J. Biol. Chem.* **2011**, *286* (9), 7379–7388.
(10) Patel, P.; Harris, R.; Geddes, S. M.; Strehle, E. M.; Watson, J. D.; Bashir, R.; Bushby, K.; Driscoll, P. C.; Keep, N. H. Solution Structure of the Inner DysF Domain of Myoferlin and Implications for Limb Girdle Muscular Dystrophy Type 2B. *J. Mol. Biol.* **2008**, *379* (5), 981–990.
(11) Lek, A.; Lek, M.; North, K. N.; Cooper, S. T. Phylogenetic Analysis of Ferlin Genes Reveals Ancient Eukaryotic Origins. *BMC Evol. Biol.* **2010**, *10* (1).
(12) Doherty, K. R.; Cave, A.; Davis, D. B.; Delmonte, A. J.; Posey, A.; Earley, J. U.; Hadhazy, M.; McNally, E. M. Normal Myoblast Fusion Requires Myoferlin. *Development* **2005**, *132* (24), 5565–5575.
(13) Wolk, C. Initial in Vitro and in Vivo Characterization of the Membrane Trafficking Protein Fer1L6, Oregon State University: Corvallis, 2016.
(14) Characterization of Fer1L6 in the Mouse C2C12 Cell Line. **2015**.
(15) Doherty, K. R.; Demonbreun, A. R.; Wallace, G. Q.; Cave, A.; Posey, A. D.; Heretis, K.; Pytel, P.; McNally, E. M. The Endocytic Recycling Protein EHD2 Interacts with Myoferlin to Regulate Myoblast Fusion. *J. Biol. Chem.* **2008**, *283* (29), 20252–20260.

(16) Ledig, S.; Röpke, A.; Wieacker, P. Copy Number Variants in Premature Ovarian Failure and Ovarian Dysgenesis. *Sex. Dev. Genet. Mol. Biol. Evol. Endocrinol. Embryol. Pathol. Sex Determ. Differ.* **2010**, *4* (4–5), 225–232.
(17) Marty, N. J.; Holman, C. L.; Abdullah, N.; Johnson, C. P. The C2 Domains of Otoferlin, Dysferlin, and Myoferlin Alter the Packing of Lipid Bilayers. *Biochemistry* **2013**, *52* (33), 5585–5592.
(18) Moghadam-Kamrani, S. J.; Keyomarsi, K. Synchronization of the Cell Cycle Using Lovastatin. *Cell Cycle* **2008**, *7* (15), 2434–2440.
(19) Martínez-Botas, J.; Ferruelo, A. J.; Suárez, Y.; Fernández, C.; Gómez-Coronado, D.; Lasunción, M. A. Dose-Dependent Effects of Lovastatin on Cell Cycle Progression. Distinct Requirement of Cholesterol and Non-Sterol Mevalonate Derivatives. *Biochim. Biophys. Acta* **2001**, *1532* (3), 185–194.

Table 1. Primer names and their sequences

Primer Number		Sequences
1141	B-actin (Forward)	AAATCGTGCGTGACATCAAA
1142	B-actin (Reverse)	AAGGAAGGCTGGAAAAGAGC
1169	Dys (Forward)	CCAGCTCTCCAACGTACTGC
1170	Dys (Reverse)	GCCAAACTGGCGATTATCAA
1446	Fer6C2A (Forward)	TACTTCCAATCCAATGCAATGTTTGGGC TGAAGGTGAAGAAGAAGA
1447	Fer6C2A (Reverse)	TTATCCACTTCCAATGTTACACCAGCTG GCGAGCC
1448	Fer6C2B (Forward)	TACTTCCAATCCAATGCAGAGGTCAGAT CCCAAAATTATCAAATTGCCATAACC
1449	Fer6C2B (Reverse)	TTATCCACTTCCAATGTTATTGGTTGTAC ACGGTCCCCAG
1450	Fer6C2C (Forward)	TACTTCCAATCCAATGCACCACTGGAGA GACCGTGGG
1451	Fer6C2C (Reverse)	TTATCCACTTCCAATGTTACTTCAGGTCA ATGAAATGGGTTGCCAG
1452	Fer6C2D (Forward)	TACTTCCAATCCAATGCACTGCTCTACC AAGAACAGCATGTTTTTCAG
1453	Fer6C2D (Reverse)	TTATCCACTTCCAATGTTAAGCCAGCTT CACAACAGGAGC
1454	Fer6C2E (Forward)	TACTTCCAATCCAATGCAGTGCAGCTCC TCTCTGTGGATC
1455	Fer6C2E (Reverse)	TTATCCACTTCCAATGTTAACACAAAAA CTGCTTCAAGTAGTTGATGGTGTA
1456	Fer6C2F (Forward)	TACTTCCAATCCAATGCACCGCCCAATC ACCCTGTCA
1457	Fer6C2F (Reverse)	TTATCCACTTCCAATGTTAGCTGTAGAA GCGGTTCTCCAGG
2197	Cyclin A2 (Forward)	GGCTGACACTCTTTCCG
2198	Cyclin A2 (Reverse)	CTGGTAGCAAGAATTAGAGCAT
2238	MyoD (Forward)	CTGCCTGTCCAGCATAGT
2239	MyoD (Reverse)	TCTGTGTCGCTTAGGGATG
2244	Cyclin B1 (Forward)	GAGGAAGAGCAGTCAGTTAGA
2245	Cyclin B1 (Reverse)	TCTCCTGAAGCAGCCTAAAT
2246	Cyclin B2 (Forward)	GCTTACACCAGTTCCCAAATC
2247	Cyclin B2 (Reverse)	TGTTCAACATCCACCTCTCC
2250	Cyclin E1 (Forward)	ATCAGTGGTGCGACATAGAG
2251	Cyclin E1 (Reverse)	CTGGATGTTGTGGGAGTCTT
2258	Cyclin E2 (Forward)	GCATTCTAGCCATCGACTCT

2259	Cyclin E2 (Reverse)	ACCATCCAGTCTACACATTCC